RSC Advances

PAPER

Cite this: *RSC Adv.*, 2023, **13**, 34576

Study on aging behavior of polyethylene glycol under three wavelengths of ultraviolet light irradiation†

Mingyu Shang,‡[a] Yanfei Wei,‡[b] Herong Zhou, *[a] Tao Wu,[a] Ke Wang,[a] Hongxiang Chen,[c] Beisong Fang[d] and Yang Zhao[d]

PEG2000 (polyethylene glycol, molecular weight: 2000) is commonly used for the dehydration and reinforcement of waterlogged wooden cultural relics, but its photo-aging degradation will seriously affect the long-term conservation of the wooden cultural relics. In this study, the photo-aging characteristics and mechanisms of PEG2000 under UV (ultraviolet) irradiations of three wavelengths were comprehensively investigated, and the surface morphology, crystal structure, and relative molecular weight of PEG2000 were systematically characterized. The results showed that PEG2000 showed a higher gloss loss rate, carbonyl index and crystallinity, and a wider molecular weight distribution with increasing aging time, especially under the irradiation of 313 nm ultraviolet light. The evolution of the PEG2000 from surface to interior during photoaging was elucidated by SEM (scanning electron microscopy) and FTIR (Fourier transform infrared spectroscopy), and it was determined that photodegradation not only occurs on the surface of PEG2000 but also gradually extends to the interior of the sample with the prolongation of irradiation time, resulting in the transformation of the basic component unit of spherical crystals in PEG2000 from fibrous crystals to spherical particles. Based on ^{1}H-NMR (nuclear magnetic resonance spectroscopy), the photochemical reactions for the generation of degradation products were proposed, and it was found that the degradation occurred at the C–H and C–O–C bonds on the main chain, forming a large number of ester and ethoxy structures. The aging degree of PEG2000 was evaluated from the perspective of surface morphology and chemical structure by gloss and FTIR spectroscopy, and it was found that the combination of gloss loss rate and carbonyl index was more suitable to evaluate the aging degree of the sample. The relevant theoretical research will provide reliable guidance for the preservation of polyethylene glycol in waterlogged wooden cultural relics.

Received 20th September 2023
Accepted 9th November 2023

DOI: 10.1039/d3ra06407g

rsc.li/rsc-advances

1 Introduction

Polyethylene glycol (PEG) is a versatile polymer with a wide range of applications, and plays an important role in the fields of biopharmaceuticals, phase change energy storage,[1,2] industrial applications, and cultural relics protection.[3] The PEG2000 studied in this article plays an important role in the field of cultural relics protection,[4] and it is often used for dehydration and reinforcement protection of waterlogged wooden cultural relics.[5,6] It is mainly infiltrated into the wood cells, and after the wood is dehydrated; it is filled in the wood cells to strengthen the wood. The repaired wooden cultural relics are easily susceptible to environmental factors such as light, temperature, moisture, oxygen, and chemical media during storage, resulting in changes in the performance and structure of the polyethylene glycol filled in the wooden cultural relics, thus affecting the restoration and long-term preservation of the wooden cultural relics.[7] For example, the polyethylene glycol filled in the wood will precipitate and adhere to the surface of utensils, thus affecting the service life of wooden cultural relics when the ambient humidity is too high.[8] Therefore, the stability study of polyethylene glycol under various environmental conditions is of guiding significance for the restoration and long-term preservation of wooden cultural relics.

Many studies on the effects of environmental factors such as heat, oxygen, and humidity on the structure and performance of polyethylene glycol have been reported in the literature. Han *et al.*[9] found that PEG6000 would be degraded by thermal

[a]*State Key Laboratory of Refractories and Metallurgy, Wuhan University of Science and Technology, Wuhan, 430081, China. E-mail: zhouhr_9@163.com*

[b]*Institute of Cultural Relics and Archaeology of Gansu, Lanzhou 730000, China*

[c]*Hubei Key Laboratory of Coal Conversion and New Carbon Material, College of Chemical Engineering and Technology, Wuhan University of Science and Technology, Wuhan, 430081, China*

[d]*Jingzhou Cultural Relics Protection Center, Jingzhou, 434000, China*

† Electronic supplementary information (ESI) available. See DOI: https://doi.org/10.1039/d3ra06407g

‡ Co-first authors: Mingyu Shang, Yanfei Wei.

oxygen in 80 °C air, and the main product was low molecular weight esters, whose degradation mechanism was random chain break of the main chain, while PEG6000 did not degrade in vacuum. Bilen *et al.*[10] reported that a polyethylene glycol thin film gradually hydrogenated at 80% RH and changed from a semi-crystalline state to a physical gel state by using optical waveguide spectroscopy, resulting in a sharp decrease in surface refractive index and a sharp increase in thickness. At the same time, hydrogenation caused fewer ether oxygen atoms to form hydrogen bonds with water molecules, making the structure of PEG more stable than before.

Compared to thermal-oxidative aging induced by thermal energy, photo-oxidative aging is caused by chain initiation caused by ultraviolet radiant energy, which leads to a rapid photo-oxidation reaction from the beginning.[11] At the same time, the chain growth process is shorter than the thermal-oxidation reaction, which means that light has an important influence on polymer aging.[12,13] Mao *et al.* showed that the aging of polystyrene (PS) with UV irradiation under air, pure water, and seawater conditions was the most obvious in an air environment and produced a large number of oxygen-containing functional groups (C=O, C–OH, O–C=O). The photo-oxidation reaction was determined by FTIR and 2D-COS to occur on the C–H bond, which clarified the aging sequence of PS functional groups in air.[14] Yang *et al.* reported that a photo-oxidative aging reaction of P(St-*co*-BA-*co*-MMA) latex film under UV irradiation occurred on the –CH– groups, which leads to the breakage of weak cross-linked chains in the film and the destruction of the connection between the microspheres, resulting in the decrease of the toughness of the latex film.[15] Ouyang *et al.*[16] showed that the oxygen-containing functional groups, carbonyl index, and crystallinity of polyvinyl chloride (PVC) increased with the increase of ultraviolet irradiation time, and the active sites and aging sequence of functional groups were determined based on Fourier transform infrared spectroscopy analyses. However, the degradation behavior of polyethylene glycol under ultraviolet irradiation and the mechanism of influence of different wavelengths of ultraviolet light on its properties and structure has not been reported in the literature.

Light exposure in the environment, especially ultraviolet light irradiation,[17] can easily lead to the degradation of wooden cultural relics and their organic protection material, polyethylene glycol,[18,19] resulting in changes in color,[20] gloss, ductility, and strength,[21] and losing the function of protective materials.[22,23] Therefore, we used three different wavelengths of ultraviolet light to simulate the aging rate of PEG2000 under different environments (indoor, outdoor, and strong aging), evaluated the aging degree of samples comprehensively from the perspective of surface morphology and chemical structure using surface gloss loss rate and carbonyl index. During this process, the evolution of PEG2000 samples from the surface to the interior during photoaging was elucidated, and the photochemical reactions were proposed to produce degradation products of PEG2000. Based on the obtained photoaging characteristics and mechanisms of PEG2000, the aging stages were summarized. This study helps to understand the aging behavior of PEG2000 in the light environment and guides the use and long-term preservation of PEG in the protection of waterlogged wooden cultural relics.

2 Material and methods

2.1 Material

Polyethylene glycol (PEG2000) was supplied by Aladdin Reagent Co., Ltd (Shanghai, China) with a specification size of 0.1 μm particles. The PEG2000 solid particles were melted in a 59 °C water bath and cooled in an 80 mm × 10 mm × 4 mm mold to obtain fixed-size samples.

2.2 Aging experiment

UV aging experiments were carried out in accordance with ASTM G154 (Standard Practice for Operating Fluorescent Ultraviolet (UV) Lamp Apparatus for Exposure of Nonmetallic Materials). The test equipment was a fluorescent ultraviolet aging test chamber, the light source was 351 nm, 340 nm, and 313 nm ultraviolet fluorescent tubes (Q-Lab Corporation), and the test temperature was 30 ± 2 °C. The PEG2000 was evenly distributed and exposed at 45° to the horizontal 10 cm below the lamp. The samples were tested after being aged for 120 h, 240 h, 360 h, 480 h, and 600 h.

2.3 Analysis of physicochemical characteristic

The gloss of the sample surface was measured using a gloss meter (YG-60), with three different positions selected on the sample and the average value taken as the gloss value. The microscopic characteristics of PEG2000 were observed using a scanning electron microscope (SEM, FEI Quanta 650). To monitor the atomic and molecular structures of the samples, X-ray diffraction (XRD, Rigaku SmartLab SE) was employed. The surface functional groups of the aged PEG2000 were determined using Fourier transform infrared (FTIR, Nicolet iN10) spectroscopy. A portion of PEG2000 was scraped from the surface and mixed with deionized water to form a solution of 5 g L^{-1}. With α-cyano-4-hydroxycinnamic acid (HCCA) as the matrix, 0.5 μL sample solution was uniformly mixed with the matrix, and 0.5 μL mixed droplets were added to the sample stage for testing. 10 mg PEG2000 was scraped from the surface of the sample and dissolved in 0.5 mL deuterated chloroform ($CDCl_3$) to form a uniform solution, which was tested by nuclear magnetic resonance instrument (^{1}H-NMR, ADVANCE 400 MHz type).

3 Results and discussion

3.1 Morphological changes treated by UV aging

The morphological change of PEG2000 is an important feature to reflect the aging degree. Fig. 1 depicted the micromorphology under 340 nm UV irradiation for 600 h, and the morphological changes under 351 and 313 nm UV irradiation were shown in Fig. S1.† The untreated samples had relatively smooth surfaces. After UV irradiation, the surface gradually became rough and developed irregular patches (Fig. 1c). With increased aging time, these spots gradually transformed into irregular pits

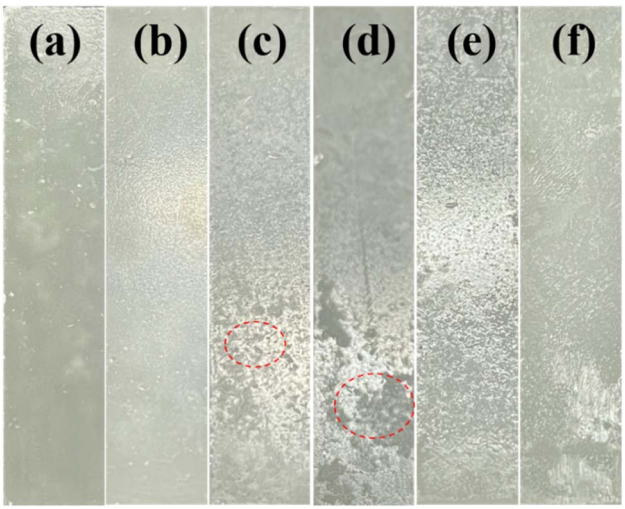

Fig. 1 Photographs of PEG2000 irradiated with 340 nm UV light for different times: (a) 0 h, (b) 120 h, (c) 240 h, (d) 360 h, (e) 480 h, and (f) 600 h.

(Fig. 1d). Finally, the surface was completely covered by irregular pits (Fig. 1f). After 351, 340, and 313 nm UV irradiation, irregular pits on the sample surface appeared at 600, 360, and 120 h, respectively. Because 351 nm ultraviolet light was relatively weak, only a small number of pits were produced on the sample's surface after irradiation for 600 h. In contrast, after 340 and 313 nm UV irradiation for the same time, most areas of the sample's surface were covered by pits. By comparing the aging characteristics of the sample surface, it is easy to find that the aging degree of PEG2000 was more serious with the increase in the test time. With the decrease in ultraviolet wavelength, the aging rate of samples increased greatly, and the aging degree of samples irradiated at 313 nm was the most serious at the same test time.

In order to study the effect of ultraviolet light on the microstructure of PEG2000, scanning electron microscopy was used to observe the morphological changes on the surface and cross-section of the sample. Fig. 2 showed the morphological changes during the irradiation of 340 nm UV light for 600 h, and the morphological changes after 351 and 313 nm UV irradiation

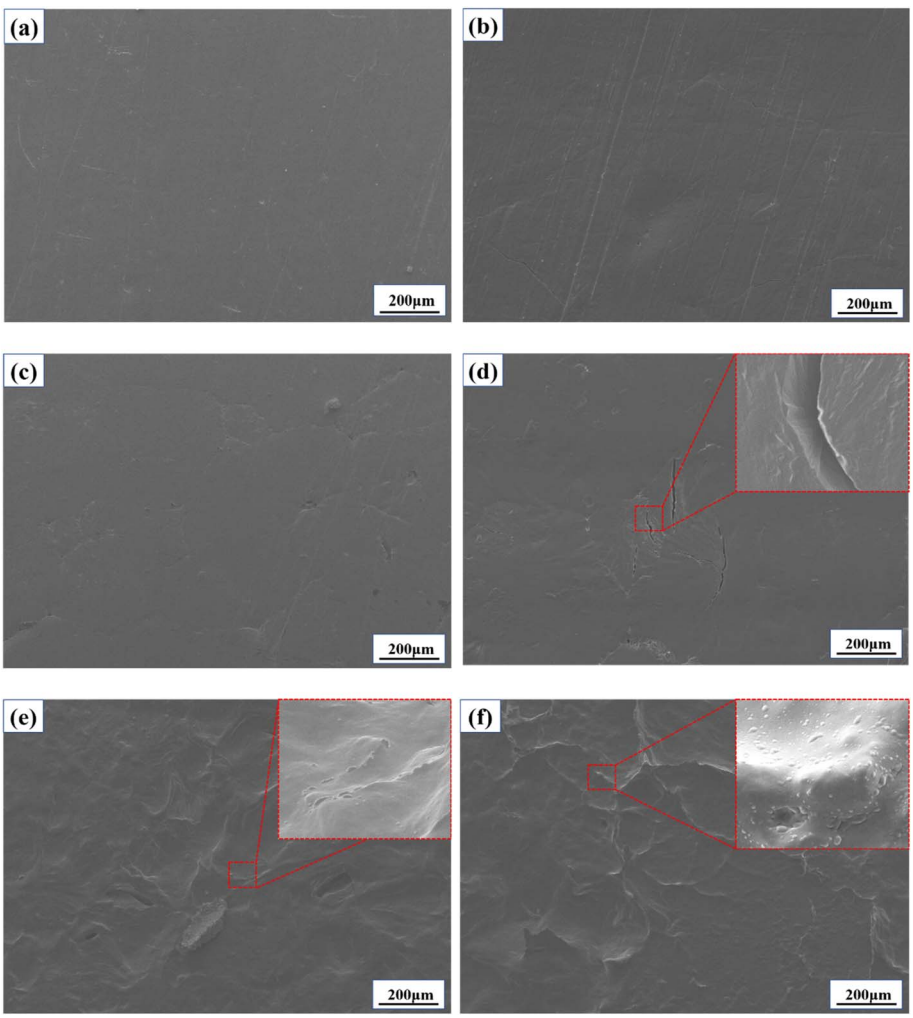

Fig. 2 SEM images of PEG2000 irradiated with 340 nm UV light for different times: (a) 0 h, (b) 120 h, (c) 240 h, (d) 360 h, (e) 480 h, and (f) 600 h.

were shown in Fig. S2.† The pristine samples in Fig. 2a had a regular and smooth surface. After exposure to UV irradiation, the surface gradually became rough and developed cracks (Fig. 2d). Several published studies have also reported the phenomenon of polymer aging under UV irradiation.[24–26] When the samples were aged to a certain extent, the surface crinkled (Fig. 2e), and bulge particles were produced (Fig. 2f). Under the irradiation of 351, 340, and 313 nm UV light, the surface cracks were observed on the surfaces at 600, 360, and 120 h, respectively. After 600 h of testing, there were only a few cracks on the surface of the sample irradiated by 351 nm ultraviolet light, irregular network texture, and a few raised particles on the surface of the sample irradiated by 340 nm, and large-scale cracks and dense raised particles on the surface of the sample irradiated by 313 nm.

Based on the macroscopic morphology shown in Fig. 1, it can be seen that the surface pits and cracks occurred at the same time. It can be deduced that the pits generated by aging on the surface are caused by cracking. With the increase of aging time, the crack number and aging degree increased, and the irregular pits gradually covered the whole surface. The bulge particles observed at the crack may be due to the precipitation of oligomers during the aging process.

Fig. 3 shows the microscopic morphology of the cross-section of the PEG2000 sample during 600 h of irradiation with 340 nm ultraviolet light. As shown in Fig. 3a, there were dense spherulites on the cross-section of the sample, with larger spherulite sizes ranging from 200 to 400 μm. The basic composition of spherulites is fibrous crystals, mainly growing radially (Fig. 3b). The red arrow in Fig. 3c shows the surface irradiated by 340 nm

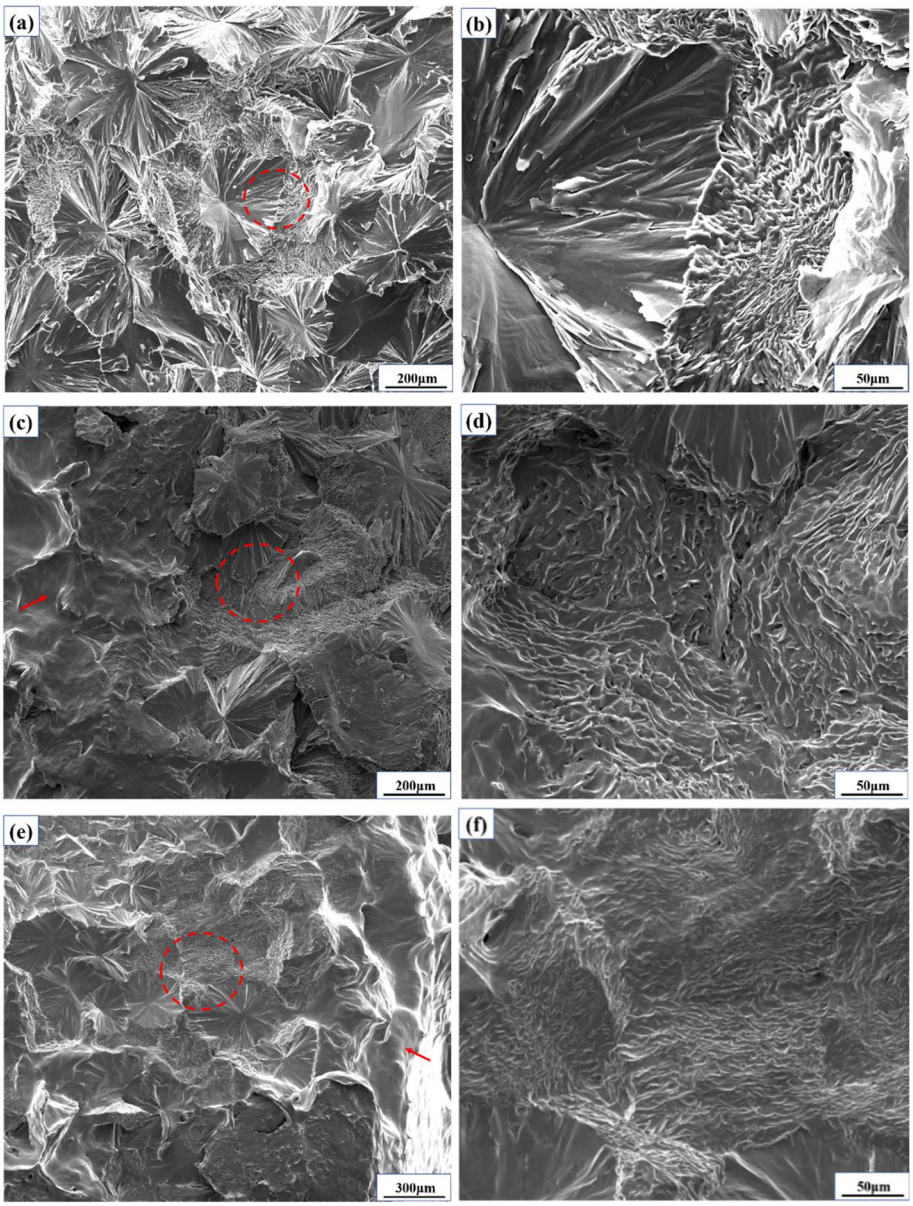

Fig. 3 Cross section microstructure of the sample after irradiation with 340 nm ultraviolet light for different times. (a) 120 h, (b) enlarged image of the red circle area in (a), (c) 480 h, (d) enlarged image of the red circle area in (c), (e) 600 h, (f) enlarged image of the red circle area in (e).

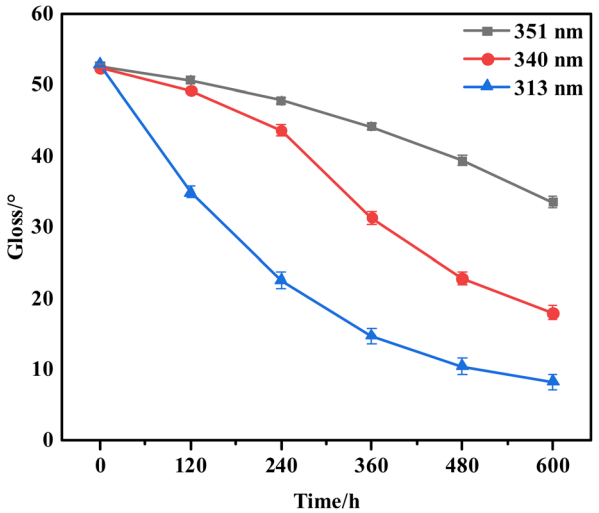

Fig. 4 The surface gloss of samples exposed to three UV irradiations for 600 h (the error bar represents the measured value of glossiness and its error range).

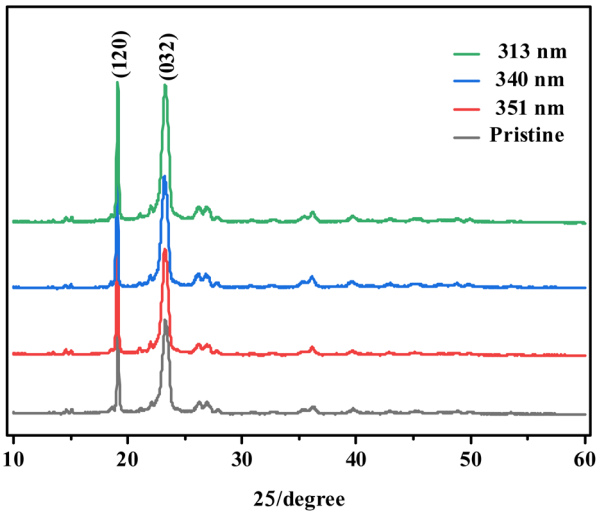

Fig. 5 XRD patterns of pristine and aged PEG2000 treated for 600 h under different UV irradiations.

ultraviolet light. At 480 hours, the surface of the sample underwent slight melting due to degradation. Fig. 3d is the enlargement of the red circle in Fig. 3c. At this time, the fibrous crystals at the end of the spherulites inside the sample were transformed into spherical particles, and the growth direction was also changed from radial to irregular. When irradiated with 340 nm ultraviolet light for 600 h, the surface of the sample at the red arrow in Fig. 3e degraded and melted severely. At this point, it is observed from Fig. 3f that the density of spherical particles increases at the cross-section of the sample. In summary, the fibrous crystals of the spherulites inside the PEG2000 gradually transform into spherical particles in the later stage of photodegradation. With increased aging time, the number of spherical particles gradually increased and continuously precipitated onto the surface of the sample, resulting in the formation of protruding particles on the surface, as shown in Fig. 2f.

In order to study the changes in surface roughness of PEG2000 under ultraviolet light, the changes in surface glossiness of the sample were monitored (Fig. 4). The initial gloss of all samples was about 52°. After 600 h irradiation with 351, 340, and 313 nm ultraviolet light, the gloss of the sample surface decreased, and the gloss loss rate of the sample surface gloss reached 36.3%, 68.9%, and 84.5%, respectively. The rate of gloss reduction changed continuously during irradiation. After irradiation with 340 nm ultraviolet light, the rate of gloss reduction first increased and then decreased, reaching the maximum value at 360 h. After 351 and 313 nm UV irradiation, the rate of gloss reduction reached the maximum value at 600 and 120 h, respectively. The lower the wavelength of UV light, the greater the gloss loss rate. At the same time, the time point corresponding to the maximum value of the rate of gloss reduction was continuously shortening.

3.2 Structural changes treated by UV aging

In order to reveal the reasons for the changes in apparent morphology and gloss caused by photoaging of PEG2000, it is necessary to further analyze from the perspective of microstructure, such as XRD, FTIR, MALDI-TOF mass spectrometry, and ^{1}H-NMR.

3.2.1 XRD analysis. In order to further analyze the crystallinity and microstructure of PEG2000 before and after aging, XRD analysis was conducted. The spectra of three kinds of PEG2000 under different UV irradiation for 600 h were recorded in Fig. 5. The peaks at 19.2° and 23.1° were assigned to the (120) crystal plane and (032) crystal plane of the monoclinic cell, respectively.[27] The diffraction-peak locations of the samples after the three UV irradiations were almost identical, and no new diffraction peak appeared, indicating that the crystalline structure was not significantly affected by the photodegradation of PEG2000. After exposure to three UV irradiations for 600 h, some sharp peaks were observed, which indicated the increase in crystallinity under different UV irradiations. The highest value of crystallinity was shown in the condition of 313 nm UV irradiation. Generally, the polymer crystallinity increases due to the destruction of its structure and functional groups after degradation.[28,29] We speculate that certain functional groups are destroyed and produced during the aging process of PEG2000.

3.2.2 FTIR analysis. In order to further verify the changes in functional groups of PEG2000 with aging time, the FTIR spectra at the surface and cross-section of the sample were displayed. The peak at 3313 cm^{-1} was attributed to the stretching vibration peak of the –O–H bond, and the peaks at 2946 cm^{-1}, 2882 cm^{-1}, and 2861 cm^{-1} were attributed to the asymmetric and symmetric stretching vibration peaks of the C–H bond in CH_2.[30] It can be observed that all spectra are similar to the one obtained for the pristine sample, with significant differences arising in the 1724 cm^{-1} region. The oxygen-containing absorption peak appeared at 1724 cm^{-1} after the different UV irradiation treatments, which belongs to the stretching vibrations of the C=O group. Besides, the carbonyl index (CI) was obtained from the absorbance ratio of carbonyl stretch (C=O) at 1724 cm^{-1} and methylene vibration (–CH_2) at 2882 cm^{-1} in

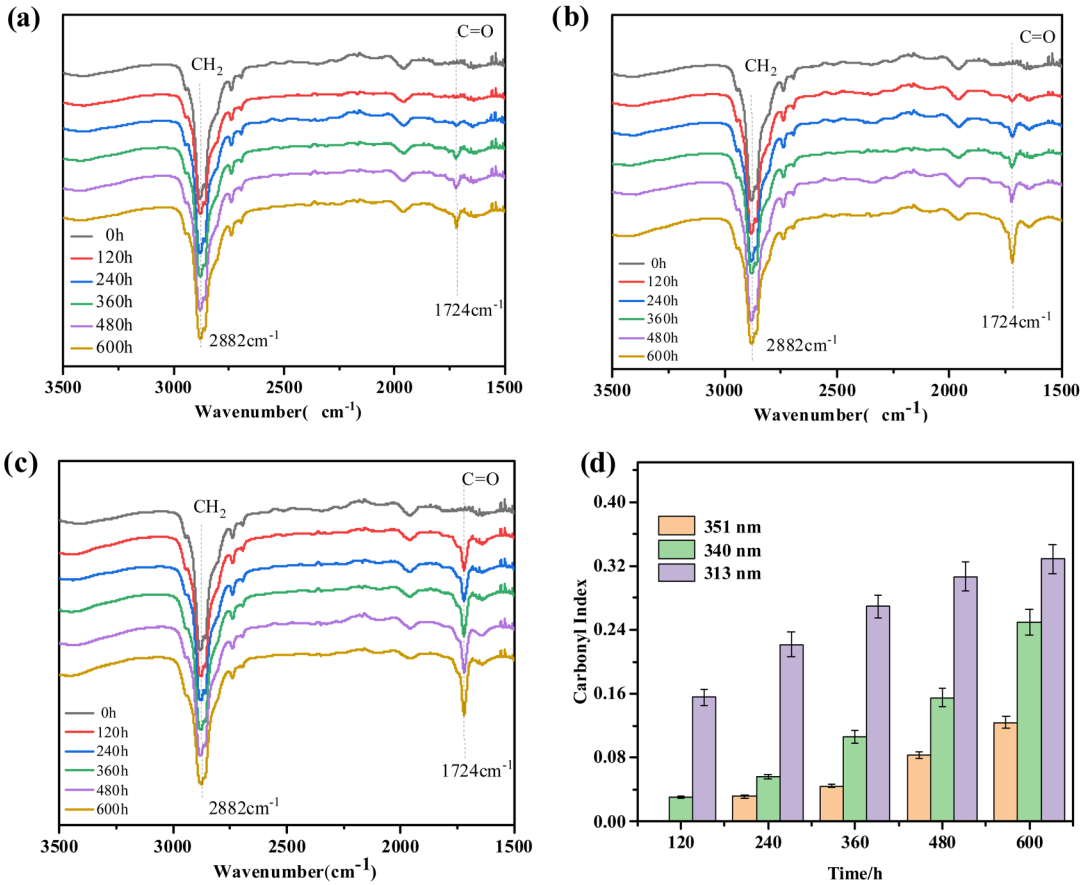

Fig. 6 FTIR spectra of PEG2000 treated by three UV irradiation with (a) 351 nm, (b) 340 nm, (c) 313 nm, and (d) the carbonyl index of aged PEG2000 treated for 600 h under different UV irradiations (the error bar represents the integral value and error range when calculating the carbonyl index of the sample).

the FTIR spectrum to reflect the degree of aging. As shown in Fig. 6d, the content of the carbonyl index increased with the increase of aging time, and the content of carbonyl stretch at the same time was maximum under 313 nm UV irradiation. Therefore, the results showed the aging effect under 313 nm UV irradiation was stronger than irradiation caused by 351 and 340 nm UV irradiation. This is consistent with the results obtained from SEM (Fig. 2).

The reason for the increase of the C=O group may be due to the C–H bond breaking on the main chain under the action of UV irradiation, reacting with oxygen to form peroxyl radical (C–O). The peroxyl radical can absorb hydrogen atoms from the surrounding environment, thus forming hydroperoxide groups (COOH), and further decomposes into the C=O group.[31,32]

In order to illustrate the changes in functional groups inside the PEG2000 sample under 340 nm ultraviolet light irradiation, we conducted infrared spectroscopy tests on the cross-section of the sample under three types of ultraviolet light irradiation for 360 hours. The results showed that after irradiation with ultraviolet light at 340 and 313 nm, the sample generated a stretching vibration peak of carbonyl group (C=O) at wave number 1724 cm^{-1}, while it was not shown at 351 nm (Fig. 7a). This indicated that 351 nm ultraviolet light did not affect the interior of the sample at 360 h, and the degradation of PEG2000 by 340 and 313 nm ultraviolet light had extended to the interior. From this, it can be seen that the photodegradation of PEG2000 not only occurs on the surface of the sample but also gradually extends from the surface to the interior over time. Fig. 7b showed the carbonyl index at the cross-section of the sample under three types of ultraviolet light irradiation for 360 h. Compared to 351 and 340 nm ultraviolet light, the relative intensity of the carbonyl index inside the sample was higher when irradiated with 313 nm ultraviolet light for 360 h, indicating that shorter wavelength ultraviolet light irradiation can accelerate the degradation process from surface to interior.

3.2.3 MALDI-TOF-MS analysis. The breakdown of chemical bonds caused by photo-aging may result in changes in the relative molecular weight, so we studied the relative molecular weight of PEG2000. As shown in Fig. 8, samples exposed to different UV light for 600 h were analyzed by MALDI-TOF. Table 1 shows the number average molecular weight (M_n), the weight average molecular weight (M_w), and the polydispersity index (PDI) of PEG2000 before and after UV irradiation. After UV irradiation for 600 h, the M_n and M_w of the samples decreased while the PDI increased, indicating that the PEG2000 molecules gradually broke down during UV degradation. The decrease in

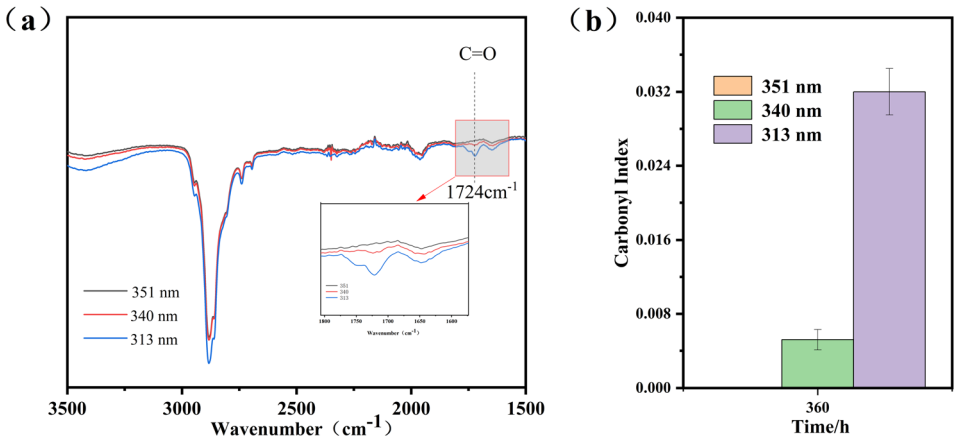

Fig. 7 Infrared spectra and carbonyl index at the cross-section of PEG2000 sample under 360 hours of irradiation with three types of ultraviolet light: (a) FTIR, (b) carbonyl index (the error bar represents the integral value and error range when calculating the carbonyl index of the sample).

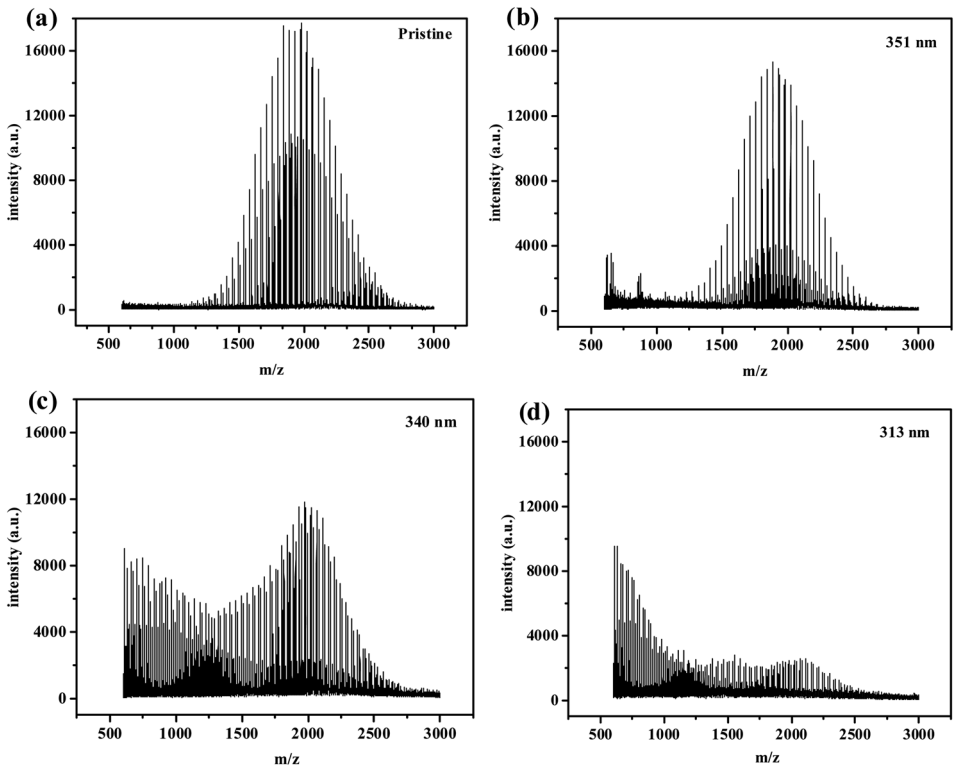

Fig. 8 MALDI-TOF spectra of pristine and aged PEG2000 treated for 600 h under different UV irradiations: (a) pristine, (b) 351 nm, (c)340 nm, and (c) 313 nm.

M_n and M_w for PEG2000 was greatest under 313 nm UV irradiation, indicating that the degree of degradation in 313 nm is higher than that in 351 and 340 nm. This is consistent with the SEM and FTIR test results.

3.2.4 ^{1}H-NMR analysis. The FTIR and MALDI-TOF analysis showed that the chemical structure of PEG2000 changed under UV irradiation. In order to infer how the chemical bonds were broken, ^{1}H-NMR was used to analyze the initial sample, and the PEG2000 sample was irradiated at three wavelengths, as shown in Fig. 9. The chemical shifts of the spectrum are attributed: the peak at 1.24 is the end-group proton at the PEG2000 capping, and the strong peak at 3.63 is the methylene proton peak on the main chain.[33] As the hydrogen on the hydroxyl group is more active, it displaces with the deuterium in deuterated chloroform, changing the position of the peak and broadening or even disappearing the peak shape. After irradiation with three UV lights, the structures of the oxidation products are listed in Table 2. The new peaks generated by degradation appear at 1.23, 2.03, and 3.71. The triple peak at 1.23 and the quadruple peak at 3.71 corresponded to the methyl and methylene protons

Table 1 Changes in molecular weight of PEG2000 treated for 600 h under different UV irradiations

Sample	M_n/Da	M_w/Da	PDI
Pristine	1955	1990	1.01
351 nm	1899	1941	1.02
340 nm	1611	1779	1.10
313 nm	1211	1478	1.22

Table 2 ^{1}H-NMR characterization of degradation products of PEG2000

No.	Degradation products	NMR characterization
A	$\overset{a}{OH}\text{-}(CH_2\text{-}CH_2\text{-}O)_n\text{-}H$	$H_a = 3.63$
B	$\overset{a}{CH_2}\overset{}{CH_2}\overset{}{O}\overset{O}{\overset{\|}{C}}\overset{b}{CH_3}$	$H_a = 3.63$, $H_b = 2.03$
C	$\overset{c}{CH_3}\overset{d}{CH_2}O$	$H_c = 1.23$, $H_d = 3.71$

in the ethoxy structure (C). The peak at 2.03 is attributed to the methyl proton attached to the ester carbonyl group in the ester group structure (B). This indicated that the photodegradation of PEG2000 generated the ester and ethoxy structures.

3.3 Discussion of photoaging behavior and mechanism

The structure and properties of PEG2000 samples did not change significantly at the initial stage of ultraviolet irradiation. For example, the FTIR did not change when irradiated with 351 nm UV light for 120 h. The SEM image showed that the surface remained smooth and flat, and the sample gloss changed little. This is because PEG2000 molecules gradually absorbed and accumulated UV radiation energy at the initial stage of UV irradiation, and the low quantum yield had not yet caused changes in structure and morphology. We call it the induction period. After the samples had been irradiated with UV light for a certain amount of time, the FTIR showed the appearance of the C=O absorption peak and a decrease in relative molecular weight. The surface of the samples exhibited obvious aging phenomena such as roughness, cracking, and a significant decrease in gloss. These phenomena are due to molecular chain scission caused by the photo-oxidation reaction of PEG2000, which we call the disruptive period. With the continuous irradiation of UV light, the morphology of the samples changed greatly. The surface of the samples formed large areas of creaking, crinkling, and irregular textures. We call it the period of acute change. With the continuous irradiation of ultraviolet light, the surface of the samples softened, appeared to large area cracking, crinkling to form irregular network lines, and was prone to adhesion. The photodegradation had expanded from the surface of the sample to the interior, resulting in the transformation of the basic component unit of

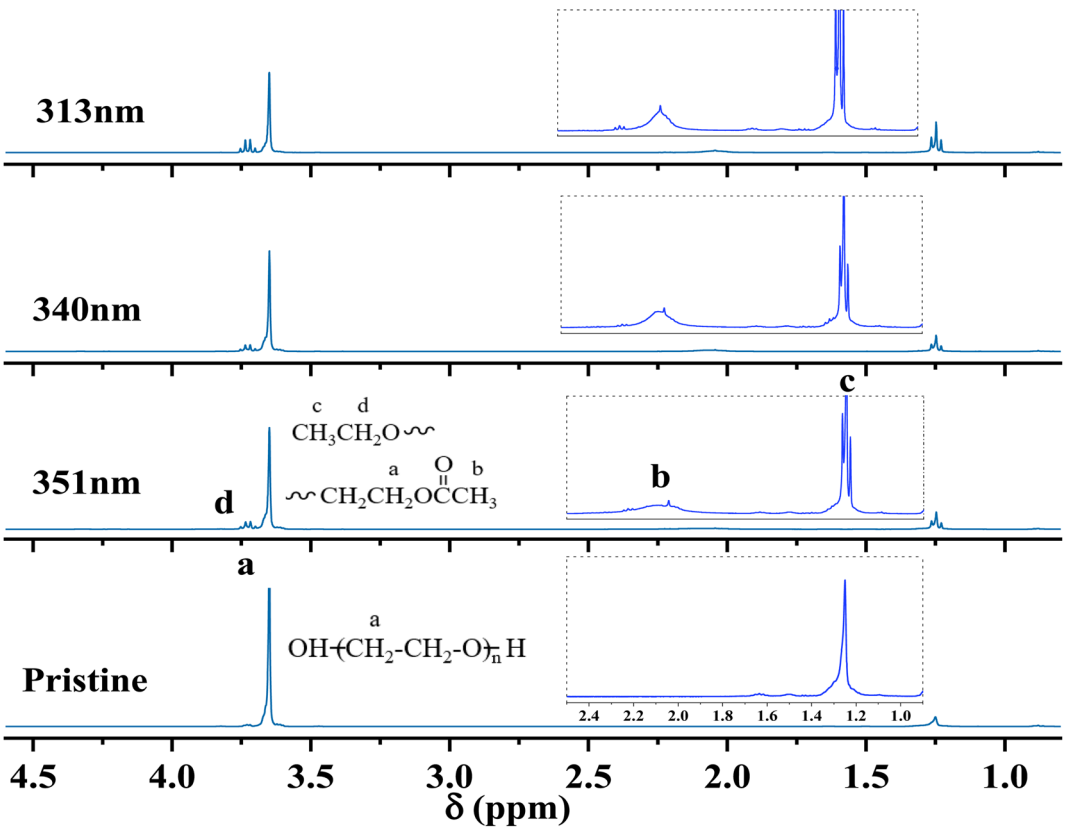

Fig. 9 ^{1}H-NMR of pristine and aged PEG2000 treated for 600 h under three UV irradiations.

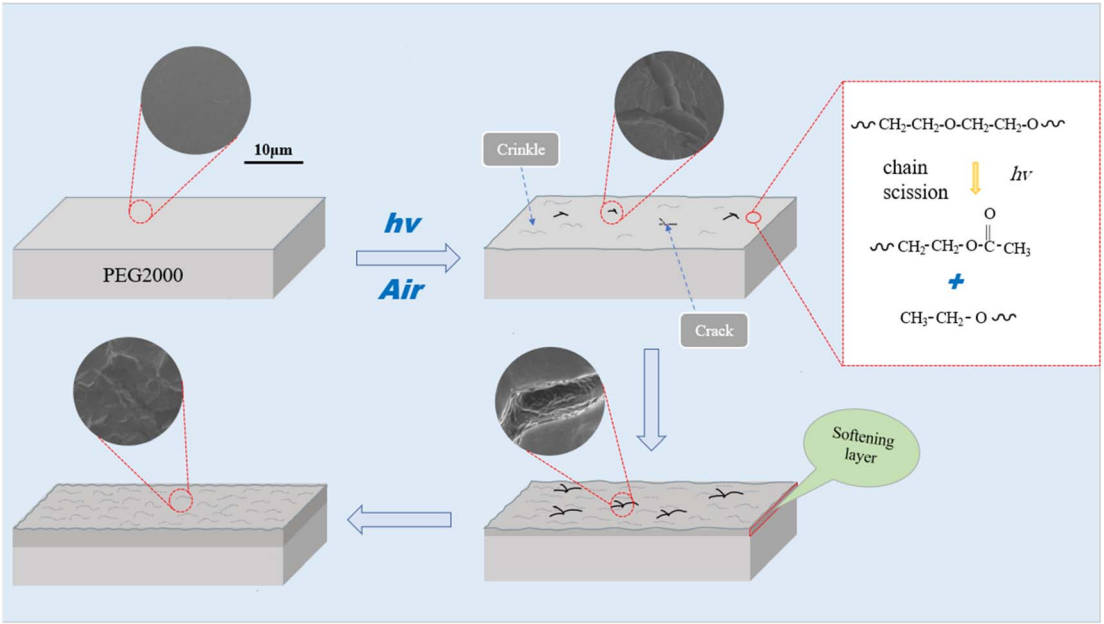

Fig. 10 Photo aging process of PEG2000 under UV irradiations.

spherical crystals inside PEG2000 from fibrous crystals to spherical particles, which we call the period of dramatic change (Fig. 10).

The aged PEG2000 exhibited a higher gloss loss rate, particularly under 313 nm irradiation. The SEM image (Fig. 2) showed that the sample's surface gradually became rough and cracked during the aging process, and the surface was covered with irregular mesh texture at the later stage of aging. The gloss can be attributed to surface aspects of PEG2000, such as the roughness.[34] Changes in surface aspects of samples, such as cracked surfaces or higher surface texture, increased the scattering of the reflected light, and lower gloss ratings were expected to be measured.[35,36] It was also found that there was a maximum value for the rate of gloss reduction on the surface of the samples when exposed to UV irradiation. As the wavelength of ultraviolet light decreased, the time corresponding to the maximum value continued to shorten. Combined with the SEM image, it was found that the maximum value of the rate of gloss reduction was located at the time when surface cracking occurred. The surface cracking phenomenon was due to the degradation of PEG2000 under UV irradiation, and the cracks caused by the photochemical reaction required a certain accumulation of UV radiation energy. Generally, the higher the energy of ultraviolet light with shorter wavelengths, the shorter the time it takes to complete energy accumulation, resulting in a phenomenon of continuously shortening the time corresponding to the maximum value of the rate of gloss reduction.

The carbonyl index can reflect the aging degree of materials to a certain extent.[37,38] Combining the changes in carbonyl index and gloss loss rate of PEG2000 samples during the three UV irradiations for 600 h (Fig. 11), it can be found that there is a good correlation between the two, especially in the 351 and 313 nm UV irradiation. As shown in Fig. 2, the sample is in a slight aging state from the induction period to the destruction

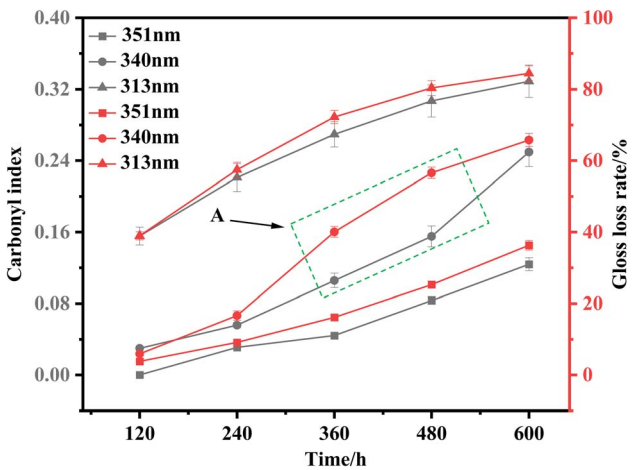

Fig. 11 Carbonyl index and gloss loss rate of PEG2000 under three UV irradiations (the error bar represents the error range of the gloss loss rate and carbonyl index).

period under the irradiation of 351 nm ultraviolet light, and the sample is in the middle and late aging stage from the destruction period to the drastic change period. This means that the variation of the sample morphology is relatively stable under the conditions of 351 and 313 nm ultraviolet light. Since the carbonyl index and gloss loss rate of the samples increased moderately during the 351 and 313 nm ultraviolet light for 600 h, this is consistent with their morphology changes, so there is a good correlation between the carbonyl index and the gloss loss rate. However, cracking and crinkling occurred on the surface of the samples during 360–480 h irradiation with 340 nm UV light, with a large degree of morphological change. The carbonyl index of samples in the range of 360–480 h increased slowly, from 0.11 to 0.15. As a result, the carbonyl index of the samples under the

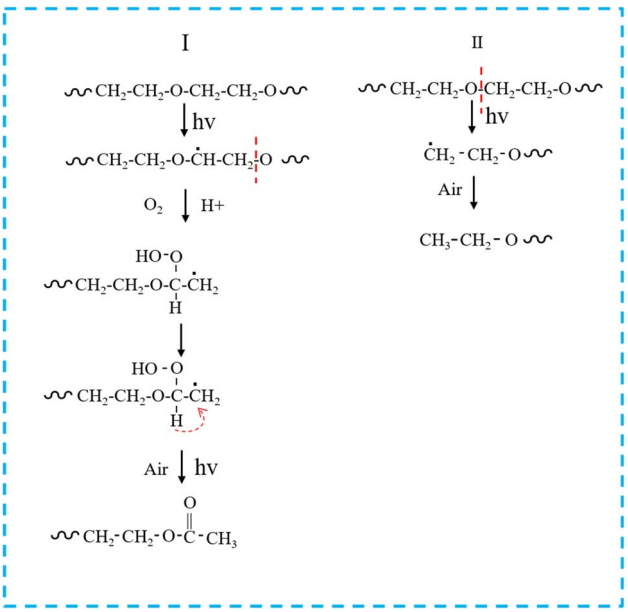

Fig. 12 Chain breaking modes I and II generated by PEG2000 photodegradation products.

condition of 340 nm cannot reflect the aging degree of the samples well, so the correlation decrease phenomenon shown in area A appears. When the surface morphology of the PEG2000 sample changes drastically in a short period of time, the change in glossiness can better reflect the aging degree of the sample. In the initial stage of aging, when the transition from the induction period to the destruction period, since there is no obvious aging phenomenon on the surface of the sample, it may be more accurate to use the carbonyl index to reflect the aging degree. In summary, this experiment uses the combination of carbonyl index and gloss loss rate and can better evaluate the aging degree of PEG2000 samples after 351 and 313 nm UV irradiation from the perspective of surface morphology and chemical structure.

Based on ^{1}H-NMR, the photochemical reactions for generating degradation products were proposed (Fig. 12). The degradation of PEG2000 occurred at both the C–H bond and ether bond (C–O–C) on the main chain. The C–H bond on the main chain of PEG2000 was broken under the action of ultraviolet light and reacted with oxygen to form a peroxyl radical (C–O). Peroxyl radical absorbed hydrogen atoms from the surrounding environment to form hydroperoxide (COOH) and then further decomposed into C=O groups. At the same time, the "C–O" in the ether bond (C–O–C) was broken to form a radical under UV light, which absorbed the H in the orthocarbon to form a methyl structure attached to the ester carbonyl group and the ester group structure was formed through the above change process (Fig. 12I).

As shown in Fig. 12II, PEG2000 degradation under UV light irradiation also occurred in another chain-breaking mode. The breakage of the PEG2000 molecular chain due to UV degradation was random, and the "O–C" in the ether bond was broken to form a radical, which ultimately formed the ethoxy groups by absorbing hydrogen atoms from the surrounding environment.

The above test results showed that polyethylene glycol was vulnerable to the influence of ultraviolet light in the environment, the loss of light and structural degradation, resulting in the change of its surface morphology and performance degradation, and then reduced or even loss the reinforcement protection of wooden cultural relics. Therefore, polyethylene glycol is used as a kind of protective material for the restoration of wooden cultural relics. In particular, it is necessary to pay great attention to the influence of ultraviolet light in the long-term preservation process of wooden cultural relics repaired by polyethylene glycol and try to preserve them in a very low or no ultraviolet light environment.

4 Conclusions

The aging of PEG2000 under three wavelengths of ultraviolet light irradiation was studied to improve understanding of PEG2000 in the protecting of waterlogged wooden cultural relics. The results showed that the aged PEG2000 underwent melting and cracking, exhibiting a higher gloss loss rate, carbonyl index, crystallinity, and wider molecular weight distribution. From this, it can be seen that photodegradation can affect the reinforcement and protection effect of PEG2000 on waterlogged wooden cultural relics. We elucidated the evolution of PEG2000 samples from surface to interior during photodegradation using SEM and FTIR and found that shorter wavelengths of ultraviolet light accelerate this process. The structure of the degradation product of PEG2000 was determined based on ^{1}H-NMR, and the photochemical reactions were proposed to produce the degradation product. Finally, we found that the method of combining surface gloss loss rate and carbonyl index is suitable for evaluating the degree of aging of samples.

Data availability

Data will be made available on request.

Author contributions

Mingyu Shang: conceptualization, methodology, software operation, investigation, data analysis, writing-original draft; Yanfei Wei: conceptualization, methodology, software operation, investigation, data analysis, writing-original draft; Herong Zhou: conceptualization, funding acquisition, resources, supervision, writing-review & editing, visualization, investigation; Tao Wu: conceptualization, data analysis, investigation; Ke Wang: resources, supervision; Hongxiang Chen: conceptualization, data analysis, investigation; Beisong Fang: material supply, resources, supervision; Yang Zhao: experimental guidance.

Conflicts of interest

The authors declare that they have no known competing financial interests or personal relationships that could have appeared to influence the work reported in this paper.

Acknowledgements

This work was financially supported by the National Key R&D Program of China, No. 2019YFC1520400.

References

1 G. T. Nguyen, *RSC Adv.*, 2023, **13**, 7621.
2 S. Liu, S. Peng and B. Zhang, *RSC Adv.*, 2022, **12**, 9587.
3 G. Cavallaro, S. Milioto and F. Parisi, *ACS Appl. Mater. Interfaces*, 2018, **10**, 27355.
4 L. Liu, L. Zhang and B. Zhang, *J. Cult. Herit.*, 2019, **36**, 94.
5 Y. Liu, J. Shi and W. Leng, *Forests*, 2022, **13**, 1204.
6 A. Vorobyev, D. N. Van, P. Kristofer and E. Gamstedt, *Mech. Time-Depend. Mater.*, 2019, **23**, 35–52.
7 R. C. Fierascu, E. Sassoni and A. C. Ion, *Front. Mater.*, 2021, **8**, 719685.
8 T. Meints, C. Hansmann and A. Gindl, *Polymers*, 2018, **10**, 81.
9 S. Han, C. Kim and D. Kwon, *Polymer*, 1997, **38**, 317–323.
10 B. Bilen, Y. Skarlatos and G. Aktas, *J. Appl. Phys.*, 2007, **102**, 073534.
11 J. C. Zhao, J. L. Yang and H. Yang, *China Plast. Ind.*, 2015, **43**, 87–92.
12 W. C. Qiu, X. D. Yang and X. Ding, *J. Text. Res.*, 2010, **31**, 33–38.
13 M. Y. Wu, *Chin. Polym. Bull.*, 2006, **4**, 76–83.
14 R. Mao, M. Lang and X. Yu, *J. Hazard. Mater.*, 2020, **393**, 122515.
15 L. Yang, D. An and T. J. Wang, *Chem. Eng. Technol.*, 2017, **40**, 1611–1618.
16 Z. Ouyang, Z. Zhang and Y. Jing, *Gondwana Res.*, 2022, **108**, 72–80.
17 H. H. G. Jellinek, *Pure Appl. Chem.*, 1962, **4**, 419–458.
18 W. He, J. Ou and F. Wang, *Colloids Surf., A*, 2023, **662**, 130949.
19 H. Yuan, X. H. Bai and H. H. Zhao, *Special Structures*, 2017, **34**, 19–24.
20 I. S. Kim, H. Cho and K. S. Sohn, *Eng. Failure Anal.*, 2021, **129**, 105719.
21 P. Malanowski, S. Huijser and F. Scaltro, *Polymer*, 2009, **50**, 1358–1368.
22 C. Q. Chen, D. M. Ke and T. Zheng, *Ind. Eng. Chem. Res.*, 2016, **55**, 597–605.
23 Y. Hu, L. Yan and B. Yue, *Chem. Phys.*, 2021, **541**, 111049.
24 J. Brandon, M. Goldstein and M. D. Ohman, *Mar. Pollut. Bull.*, 2016, **110**, 299–308.
25 J. Lin, D. Yan and J. Fu, *Water Res.*, 2020, **186**, 116360.
26 C. C. Tang, H. I. Chen and P. Brimblecombe, *Mar. Pollut. Bull.*, 2018, **133**, 392–401.
27 R. Li, Y. Wu and Z. Bai, *RSC Adv.*, 2020, **10**, 42120–42127.
28 G. Liu, Z. Zhu and Y. Yang, *Environ. Pollut.*, 2019, **246**, 26–33.
29 M. T. Taghizadeh, R. Abdollahi and N. S. Orang, *J. Polym. Environ.*, 2012, **20**, 208–216.
30 M. T. Caccamo and S. Magazù, *Polym. Test.*, 2017, **62**, 311–318.
31 E. Yousif and R. Haddad, *SpringerPlus*, 2013, **2**, 1–32.
32 A. Ammala, S. Bateman and K. Dean, *Prog. Polym. Sci.*, 2011, **36**, 1015–1049.
33 J. L. Pasek-Allen, R. K. Wilharm and J. C. Bischof, *ACS Omega*, 2023, **8**, 4331–4336.
34 M. Yonehara, T. Matsui and K. Kihara, *Mater. Trans.*, 2004, **45**, 1027–1032.
35 E. Scrinzi and S. Rossi, *Mater. Des.*, 2010, **31**, 4138–4146.
36 G. F. Tjandraatmadja, L. S. Burn and M. C. Jollands, *Polym. Degrad. Stab.*, 2002, **78**, 435–448.
37 Y. Zhang, Y. Peng and C. Peng, *Environ. Sci. Technol.*, 2021, **55**, 13802–13811.
38 C. Campanale, I. Savino and C. Massarelli, *Polymers*, 2023, **15**, 911.